

R. Ya. Stetsiv, O. Vorobyov

Phase Diagrams of Ion Conductor

*Institute for Condensed Matter Physics National Academy of Sciences of Ukraine
1 Sviatsitskii Str., Lviv, UA-79011, Ukraine, E-mail: stetsiv@icmp.lviv.ua*

Equilibrium states of one-dimensional ion conductor are investigated on the bases of the lattice model where ions are treated as Pauli particles. The frequency dependencies of single-particle spectral densities are calculated using exact diagonalization technique for the finite ion chain and diagrams of states are obtained analyzing the features of this spectra. The regions of existence of various phases are obtained.

Keywords: Pauli particles, ion conductor, spectral density, phase diagrams.

Стаття поступила до редакції 13.02.2013; прийнята до друку 15.03.2014.

Introduction

An important problem of modern physics, which is of great interest from both experimentalists and theorists is to study phenomena in systems with ion and proton conductivity. Attention to these systems is paid due to ever-increasing possibilities of practical applications - as a solid electrolyte in capacitors and batteries, in membranes of fuel cells, in electronics, control and signalling [1] devices for special purposes. Therefore new compounds with high ionic conductivity were synthesized recently in order to find materials stable against chemical and mechanical action and with other specific properties. As an example, we can cite a series of lithium conductive materials synthesized from perovskite structures [2, 3, 4]. Just recently a new superionic crystal $\text{Li}_{10}\text{GeP}_2\text{S}_{12}$ which conductivity reaches $12 \text{ m}\Omega^{-1}\text{cm}^{-1}$ at room temperature and $0.41 \text{ m}\Omega^{-1}\text{cm}^{-1}$ even at -30°C is synthesized [5]. The conductivity of ionic conductors is particularly high when a number of ions is much less than a number of positions in a lattice, i.e. when there are vacancies. Therefore a lot of free positions facilitates ion hopping probability from one position to another.

A special class of ionic conductors is represented by crystals, where charge carriers are hydrogen ions (protons). At low temperatures, they are ferroelectric or ferroelastic crystals, but at higher temperatures they undergo transition to superprotonic phase, while the conductivity is increased by several orders of magnitude (among others there are compounds of the general form MeHXO_4 , where $\text{M} = \text{Cs, Rb, NH}_4$; $\text{X} = \text{S, Se}$). Numerous structural studies have shown that in low-temperature phase the ions (protons) are clearly in the fixed positions, while in high-temperature phase they are

distributed with equal probability between multiple positions in the unit cell. Lattice model are widely used for a theoretical description of ion and proton transport at the microscopic level. They are either based on Fermi statistics [6-10] or on "mixed" Pauli statistics [11-14], which particles are of Bose nature, but they also obey the Fermi rule. Charge transfer process in some superionics occurs along the chain (one-dimensional) structures. Examples are the proton conductor $\text{LiN}_2\text{H}_5\text{SO}_4$ [15], some superionic (superprotonic) conductors, in particular CsHSO_4 [16], coordination polymers like iron oxalate dihydrate $\text{Fe}(\text{C}_2\text{O}_4) \cdot 2\text{H}_2\text{O}$, nanotubes [17], etc.

In this paper, we investigate the equilibrium states of one-dimensional ionic Pauli conductor based on the lattice model, which takes into account the ion hopping, internal modulating field and short-range interactions between ions. Particular attention is paid to the latter, because according to the experimental data [18] and quantum-chemical calculations [19, 20] the short-range interactions are important in real systems and largely determines their behavior. Moreover, in the case of Pauli conductor the short-range interaction is responsible for the transition to the charge density wave (CDW)-state [21]. We investigate the transition from (CDW)-phase to the superfluid (SF)-like phase, which can be considered as analogue of superionic phase and to the Mott insulator (MI)-type phase. The calculations are performed using the exact diagonalization technique. Analyzing the ion single-particle spectral densities and their reconstruction at the change of concentration of ions, we get the state diagram of one-dimensional ionic conductor.

I. Single-particle spectral densities and regions of existence of the various phases

In previous work [22] the expressions for the spectral densities in different phases were obtained within the random phase approximation in the framework of the two-sublattice hard-core boson model. Their calculations were performed and the shape of spectral densities in different phases was determined. In this paper the spectral density is calculated by exact diagonalization technique for one-dimensional ($d = 1$) chain structure. Diagrams of states are constructed basing on analysis of features of these spectra. We take into account the conclusions of studies [12, 13, 22, 23]. In particular, in determining the regions of existence of various phases, we have used the fact that the important property of the spectral density in superfluid (SF) phase is the presence of negative branche (at $w < 0$), which merges continuously with the positive branches at the point $w = 0$ (see for example [22, 23]) where the chemical potential m is placed. It is consequence of fact, that in

SF- phase (the phase with the Bose condensate) the chemical potential goes into the Bose excited band. In contrast, in CDW-phase there is a gap between negative and positive branches. Thus we have the splitting of the spectrum into two subbands and therefore modulated state with doubled lattice period. CDW-phase at $T = 0$, characterised by the half-filling, exists. The level of the chemical potential m is located in the middle of the gap between the two bands. In Mott insulator state (MI) the commutator spectral density has branches with only one sign. The chemical potential is placed above (or below) the two bands [22]. Described above features can be seen in the Figure 1 where single-particle spectral density are obtained for different phases.

II. Model and method (exact diagonalization approach)

We consider of the one-dimensional ion conductor as the chain of heavy immobile ionic groups and light ions that move along this chain occupying certain positions. The subsystem of light ions is described with the

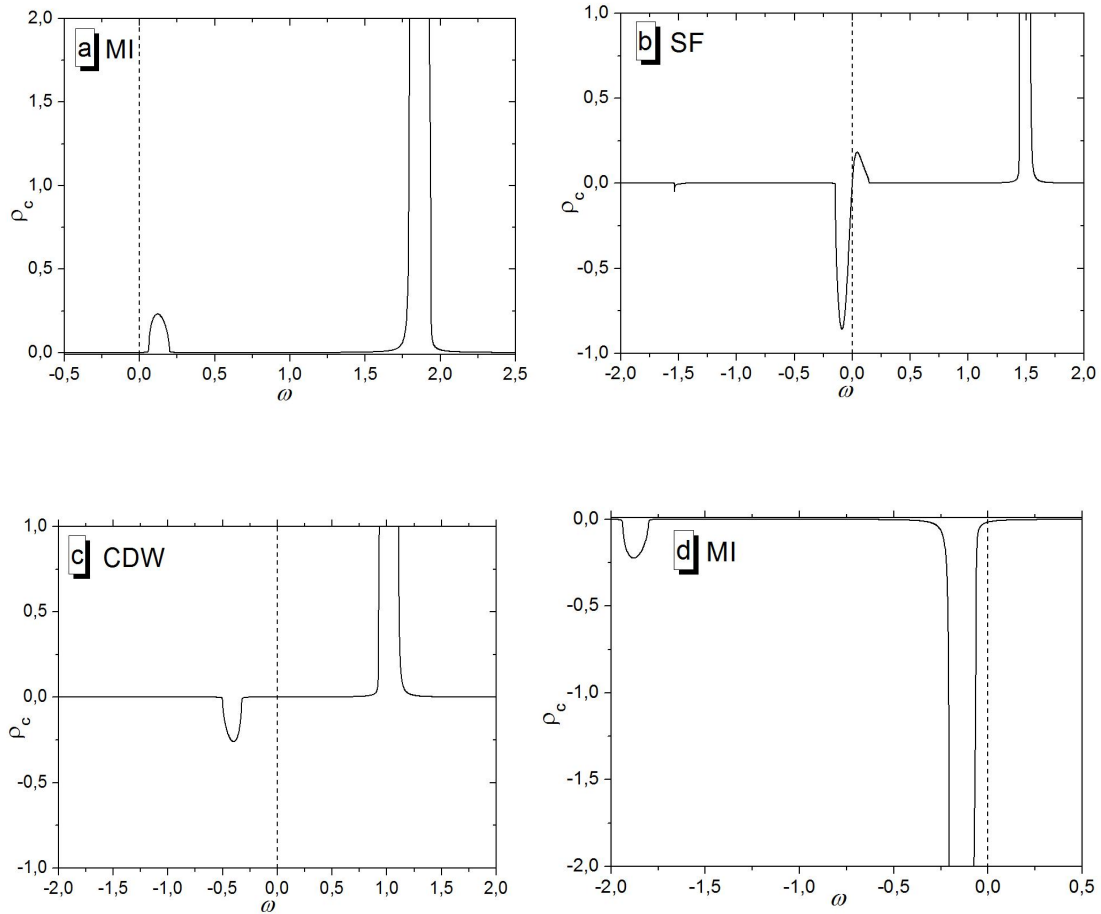


Fig. 1. Boson single-particle spectral density for different phases of two-sublattice hard-core boson model of ionic conductor [22].

following Hamiltonian

$$\hat{H} = t \sum_i (c_i^\dagger c_{i+1} + c_{i+1}^\dagger c_i) + V \sum_i n_i n_{i+1} - m \sum_i n_i + A \sum_i (-1)^i n_i. \quad (1)$$

This model takes into account the nearest-neighbour ion transfer (with hopping parameter t), interaction between ions that occupy nearest-neighbouring positions (with corresponding parameter V) and modulating field (parameter A). The system is divided into two sublattices under influence of the A field, which simulates the long-range interactions between the particles, which contributes to the modulation of the spatial distribution of light ions in the so-called ordered phase (the existence of such phases at low temperatures is characteristic features of superionic conductors). In our case $c_i (c_i^\dagger)$ are Pauli operators. They describe the process of annihilation (creation) of ion in position i therefore $n_i = c_i^\dagger c_i$ is the occupation number of protons in this position. In this case the model (1) is equivalent to the extended hard-core boson model, i.e. the boson Hubbard model with repulsive interaction between nearest neighbours and infinite on-site repulsion $U \rightarrow \infty$ [24].

For the chain of N sites we introduce the many-particle states

$$|n_1, n_2, \dots, n_N\rangle. \quad (2)$$

The Hamiltonian matrix on the basis of these states is the matrix of the order $2^N \times 2^N$. This matrix is diagonalized numerically

$$U^{-1} H U = \hat{H} = \sum_p \lambda_p X^{pp}, \quad (3)$$

where λ_p are eigenvalues of the Hamiltonian, X^{pp} are Hubbard operators. The same transformation is applied to the creation and annihilation operators

$$U^{-1} c_i U = \sum_{pq} A_{pq}^i X^{pq}, \quad U^{-1} c_i^\dagger U = \sum_{rs} A_{rs}^{i*} X^{rs} \quad (4)$$

We construct single-particle Green's function $G_{i,i} = \langle\langle c_i | c_i^\dagger \rangle\rangle$, that contains information about single-particle energy spectrum of the system. For Pauli creation and annihilation operators this Green's function can be constructed in two ways, i.e. commutator Green's function

$$\langle\langle c_i(t) | c_i^\dagger(t') \rangle\rangle^{(c)} = -i\Theta(t-t') \langle [c_i(t), c_i^\dagger(t')] \rangle \quad (5)$$

and anticommutator Green's function

$$\langle\langle c_i(t) | c_i^\dagger(t') \rangle\rangle^{(a)} = -i\Theta(t-t') \langle \{c_i(t), c_i^\dagger(t')\} \rangle. \quad (6)$$

Imaginary part of these Green's functions are the single-particle spectral densities

$$r(w) = -\frac{1}{pN} \sum_{j=1}^N \text{Im} \langle\langle c_j | c_j^\dagger \rangle\rangle_{w+ie} = -\frac{1}{pN} \sum_{j=1}^N \text{Im} \left[\frac{1}{Z} \sum_{pq} A_{pq}^j A_{pq}^{j*} \frac{e^{-bl_p} - he^{-bl_q}}{w - (l_q - l_p) + ie} \right], \quad (7)$$

where $Z = \sum_p e^{-bl_p}$. Spectral densities in (7), obtained

from commutator $h = 1$ (5) and anticommutator $h = -1$ (6) Green's functions respectively, exhibit discrete structure. They consist of some number d -peaks due to the finite size of a cluster (in our calculations the value $N = 10$ was taken). Therefore we apply the periodic boundary conditions to the cluster and introduce small parameter Δ to broaden the d -peaks according to

$$\text{Lorentz distribution } d(w) \rightarrow \frac{1}{p} \frac{\Delta}{w^2 + \Delta^2}$$

III. Ion spectral densities and diagram of states

We calculated the spectral density (7) in a wide range of values of the short-range interaction between the ions for different values of temperature and chemical

potential. Experimental studies of some specific crystals [18, 25], and quantum-chemical calculations [19] make it possible to estimate the value of the correlation constant $V = 3000 \dots 10000 \text{ cm}^{-1}$, and the value of the transfer parameter $t = 40 \dots 2500 \text{ cm}^{-1}$. This shows that in real systems there is a strong correlation between ions, which has a significant impact on the structure and energy spectrum of the system. In our work we have chosen: $V/t = 0, 1, \dots, 6$. In the following, we relate all energy parameter, including kT , to the hopping parameter t , which is taken as the energy unit.

Analyzing the shape and topology of the calculated frequency-dependent spectral densities at different values of parameters of the model we built the corresponding state diagram. When constructing diagrams we have based on the discussed above features of the spectral density in a one or another phase (see the first chapter).

When the modulating field A is present, the neighboring positions become nonequivalent and lattice

is divided into two sublattices with the different ion occupancy. Modulating field extends CDW- phase region, whereas the SF phase region decreases. Here we present the phase diagrams at $T = 0$. Figure 2 shows the phase diagrams depending on the value of short-range interactions between ions V and values of modulating field A . It is shown that in the case of the (μ', V) diagram the line of coexistence of SF and MI phases is straight (the value of the chemical potential at which the phase transition take place is proportional to V). Unlike the previous case, in the (μ', A) diagram the line that separates the CDW and SF phase is straight. For convenience we use the notation $m' = m - V$.

The gap in the spectrum of CDW phase increases with the growth of both parameters V and A . Expansion of the gap in the spectrum with increasing V was obtained in previous studies, but this was done in the case of Fermi statistics, ie, for the spinless-fermion model [10, 26]. As a whole, the width of the region of CDW phase increases with increasing magnitude of the short-range interaction V as well as the value of the modulating field A . When $V = 0$ its width is directly proportional to the strenght of modulating field A (the lines separating the CDW and SF phases are of the form: $m' = +A$ and $m' = -A$). In this regard, the diagram in [Figure 2](#) for $V = 0$ coincides with the exact diagram obtained analytically for the one-dimensional case (see

[27]), where only the case $V = 0$ was considered. The exact analytical solution in this case was possible (the Jordan-Wigner transformation that transforms the hard-core boson Hamiltonian into the non-interacting spinless-fermion Hamiltonian for one-dimensional systems was used [28]). Similar studies were performed in the [12].

Figure 3 shows the calculated commutator spectral density for some values of m' , which is related to different phases at $T = 0$. The level of chemical potential is placed in the $w = 0$ point. The mean number n for a given m was calculated according to the spectral theorem $n = \int_{-\infty}^{\infty} \frac{r_a(w)dw}{e^{bw} + 1}$, where r_a - is the anticommutator spectral density (density of states).

Figure 3 (c) refers to the CDW phase, 3 (b) - to the SF phase, when at $w = 0$ negative branch of commutator spectral density merges into positive branch with no gaps between them. Figure 3 (a) corresponds the MI phase. Here chemical potential is placed below the bottom of the lower subband; commutator spectral density has only positive branch. We have shown that at $T = 0$ the CDW phase is realized only in the case of half-filling ($n = 1/2$), and exists only in the point $m' = 0$ when $V = 0$ and $A = 0$. When anybody of these parameters is different from zero, the region of CDW

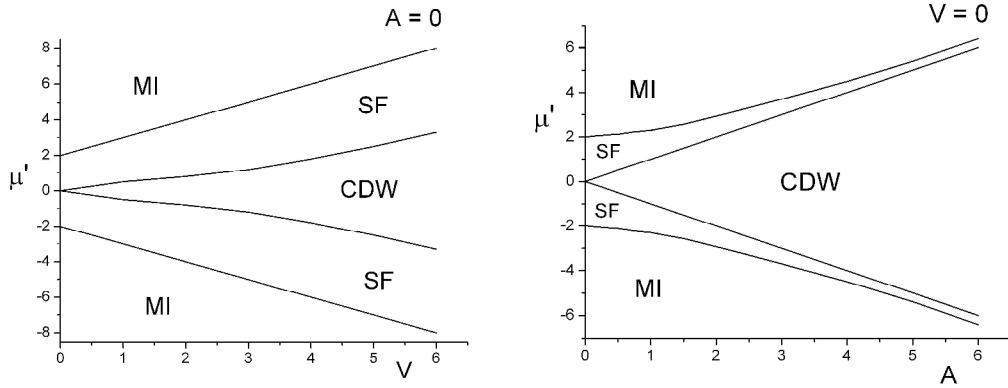


Fig. 2. Diagrams of state of one-dimensional ionic conductor in the (μ', V) and (μ', A) plains ($T = 0$).

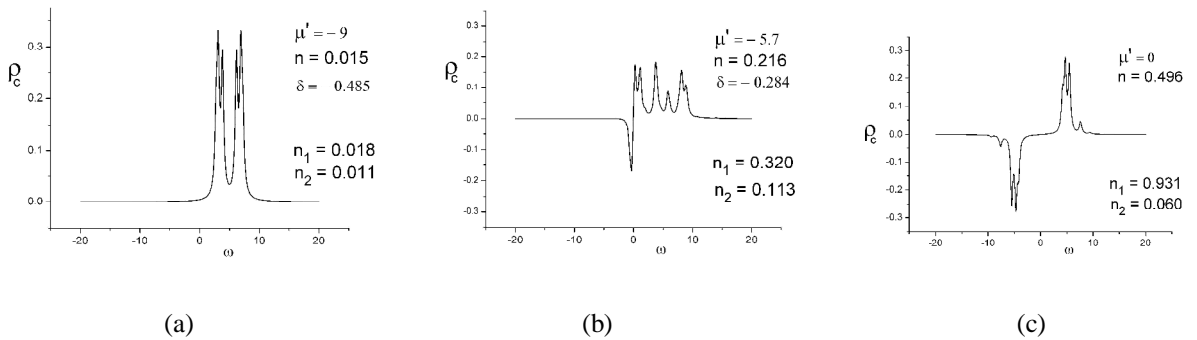


Fig. 3. Commutator single-particle spectral density of one-dimensional ionic conductor for different states at $T = 0$, $V = 4$, $A = 1$, $t = 1$, $\Delta = 0,25$. The level of the chemical potential coincides with the point $w = 0$.

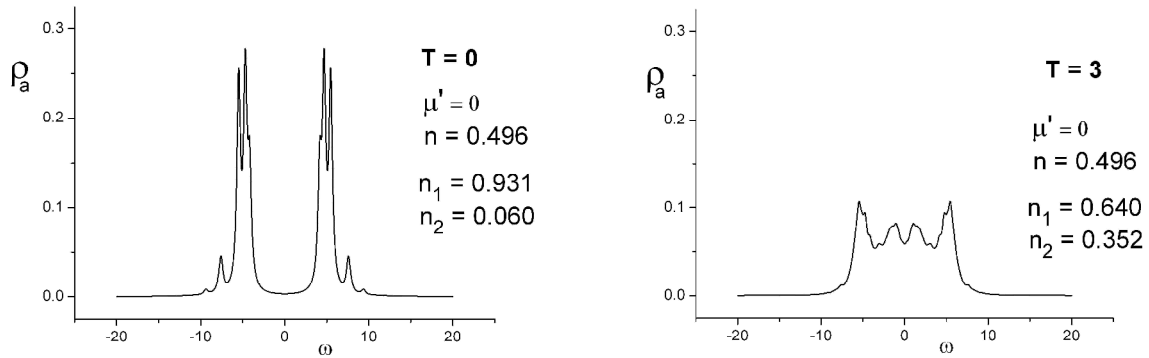


Fig. 4. Closing of the gap in the spectrum of one-dimensional ionic conductor with the increase of temperature. The case of half-filling ($n = 1/2$); $m' = 0$, $V = 4$, $A = 1$, $t = 1$. The level of the chemical potential coincides with the point of $w = 0$.

phase becomes finite (in the m' coordinates); for example, when $V = 4$, $A = 0$, we obtain: $-1,8 < m' < 1,8$

At $T \neq 0$, with increasing temperature CDW phase is eroded. We observe the effect of thermal transfer of the insulator-conductor type (the analogue of the so-called Mott transition).

The possibility of such an effect for objects that are studied in this work was shown in [29] and confirmed by numerical calculations [26] for the case when the particles are subjected to Fermi statistics. The effect can be illustrated by temperature changes of the single-particle anticommutator spectral density (density of states) (see Figure 4), calculated based on the formula (7). The gap in the spectrum ($r_a = 0$), which occurs at $T = 0$ at half filling is associated with the charge-ordered state. This is due to the repulsive short-range interactions between the particles, which forms such type of the ground state of the system. At $T \neq 0$ gap gradually closes.

Conclusions

The structure of the energy spectrum of one-dimensional ionic conductor is determined by the interaction between the ions, their concentration and

temperature. It is shown by the exact diagonalization method that at $T = 0$ the short-range repulsive interaction between ions leads to the splitting of the energy spectrum of one-dimensional ionic conductor and the appearance of the gap in the spectrum at the ionic concentration $n = 1/2$. At $T \neq 0$ a gap disappears gradually with increasing temperature. At $T = 0$ the CDW phase is present only in a half filled state. The width of the CDW phase region (as function of m) increases with the increase of magnitude of the short-range interaction V and the value of the modulating field A (the latter can be associated with an internal field arising from the long-range interactions). The gap in the spectrum of this phase also increases with increasing values of V and A . Analyzing the single-particle spectral density $r_c(w)$, calculated numerically for the one-dimensional case, we obtain the boundaries of CDW, SF, MI phase regions at $T = 0$ for different values of short-range interaction parameter and modulating field.

Стеців Р.Я. - кандидат фізико-математичних наук, старший науковий співробітник відділу квантової статистики;

Воробйов О.А. - кандидат фізико-математичних наук, науковий співробітник відділу квантової статистики.

- [1] P. Kumar, S. Yashonath, J. Chem. Sciences, 118, 135 (2006)
- [2] A. Belous, Solid State Ionics 90, 193 (1996).
- [3] A. Belous, J. European Ceramic Society 21, 1797 (2001).
- [4] A. Belous, Ionics 4 (5-6), 360 (1998)
- [5] N. Kamaya, K. Homma, Yu. Yamakawa, M. Hirayama, R. Kanno, M. Yonemura, T. Kamiyama, Yu. Kato, S. Hama. K. Kawamoto and A. Mitsui, Nature Materials 10, 682 (2011).
- [6] W. Salejda, N.A. Dzhavadov, Phys. Stat. Sol. (b) 158, 119 (1990).
- [7] I.V. Stasyuk, N. Pavlenko, B.Hilczer, Phase Transitions 62, 135 (1997).
- [8] V. V. Krasnogolovets, P. M. Tomchuk, Phys. Stat. Sol. (b) 130, 807 (1985).
- [9] I.V. Stasyuk, O. Vorobyov, B. Hilczer, Solid State Ionics 145, 211 (2001).
- [10] I.V. Stasyuk, O. Vorobyov, Phase Transitions 80, 63 (2007).

- [11] G. D. Mahan, Phys. Rev. B 14, 780 (1976).
- [12] I.V. Stasyuk, I. R. Dulepa, Condens. Matter Phys. 10, 259 (2007).
- [13] I.V. Stasyuk, I. R. Dulepa, J.Phys. Studies 13, 2701 (2009).
- [14] R. Micnas, J. Ranninger, S. Robaszkiewicz, Rev. Mod. Phys. 62, 170 (1990).
- [15] A. Pietraszko, J. Goslar, W. Hilczer and L. Szczepanska, J. Molecular Structure 688, 5 (2004).
- [16] G. Lahajnar, R. Blinc, J. Dolinsek, D. Arcon and J. Slak, Solid State Ionics 97, 141 (1997).
- [17] M. Yamada, W. Mingdeng, I. Honma and Z. Haoshen, Electrochemistry communication 8, 1549 (2006)
- [18] R. Hassan, E.S. Campbell, J. Chem. Phys. 97, 4362 (1992).
- [19] M. Eckert, G. Zundel, J. Phys.Chem. 92, 7016 (1988).
- [20] I.V. Stasyuk, R.Ya. Stetsiv, Yu.V. Sizonenko, Condens. Matter Phys. 5, 685 (2002).
- [21] I.V. Stasyuk, O. Vorobyov, R.Ya. Stetsiv, Ferroelectrics 426, 6 (2012).
- [22] I.V. Stasyuk, O. Vorobyov, Condens. Matter Phys. 16, 23005 (2013).
- [23] C. Menotti, N. Trivedi, Phys. Rev. B 77, 235120 (2008).
- [24] P. Niyaz, R.T. Scalettar, C.Y. Fong, G.G. Batrouni, Phys. Rev. B 50, 363 (1994).
- [25] W. Munch, K.D. Kreuer, U. Traub and J. Maier, Solid State Ionics 77, 10 (1995).
- [26] I.V. Stasyuk, O. Vorobyov, Ferroelectrics 376, 64 (2008).
- [27] I. Hen, M. Iskin, M. Rigol, Phys. Rev. B 81, 064503 (2010).
- [28] E. Lieb, T. Schults, D. Mattis, Ann. Phys. 16, 407 (1961).
- [29] I.V. Stasyuk, O. Vorobyov, Integrated Ferroelectrics 63, 215 (2004).

Р.Я. Стеців, О. Воробйов

Фазові діаграми іонного провідника

*Інститут фізики конденсованих систем НАН України, вул. Свєнціцького 1,
79011 Львів, Україна, E-mail: stetsiv@icmp.lviv.ua*

Досліджено рівноважні стани одновимірного іонного провідника на основі ґраткової моделі в якій іони трактуються як частинки Паулі. Методом точної діагоналізації розраховано частотну залежність одночастинкових спектральних густин для скінченних іонних ланцюжків. На основі аналізу цих спектрів отримано діаграми станів та встановлено області існування різних фаз.